Research Report

Sidewall Functionalization of Vertically Aligned Carbon Nanotubes by Alignment-preserving Methods

Riichiro Ohta, Itaru Gunjishima, Tomohiro Shimazu, Hisayoshi Oshima, Kazuma Shinozaki, Koichi Nishikawa, Tatsuya Hatanaka and Atsuto Okamoto

Report received on Oct. 5, 2012

ABSTRACT We have developed two methods for functionalizing the sidewalls of vertically aligned carbon nanotubes (VA-CNTs), which are capable of preserving the aligned morphology. The first method involves deposition of Pt nanoparticles on the sidewalls of VA-CNTs, which employs antisolvent precipitation of naphthalene particles to prevent access of adjacent CNTs through surface tension. The advantage of this method is illustrated by comparing it with a conventional solution-immersion process that caused severe agglomeration of VA-CNTs. The second method involves nitrogenation of VA-CNTs by applying pretreatment of ultraviolet light irradiation and subsequently reacting with ammonia gas, which does not use solution-immersion. This method incorporated nitrogen atoms along the sidewalls of VA-CNT without destroying the cylindrical tube structure, which has been difficult to accomplish by the frequently used process that involves synthesizing nitrogen-doped CNTs directly from precursors containing nitrogen and carbon. Spectroscopic analysis revealed that nitrogen atoms were incorporated mostly at pyridinic and pyrrolic sites. Scanning electron microscopy observations confirmed that both methods preserved the vertically aligned morphology.

KEYWORDS Carbon Nanotubes, Vertical Alignment, Agglomeration, Nitrogenation, Platinum Deposition, Antisolvent Precipitation, Ultraviolet Light Irradiation, Ammonia Treatment

1. Introduction

Carbon nanotubes (CNTs) are of great scientific and practical interest due to their outstanding properties that pertain to electronics, mechanics, optics, thermology, and various other fundamental and applied research fields.[1] Vertically aligned CNTs (VA-CNTs) have recently been attracting considerable interest due to their distinctive characteristics, such as extremely high specific surface area, low density, and anisotropy, which in conjunction with the intrinsic properties of individual CNTs make them attractive for electrical[2] and energy applications.[3] VA-CNTs have also been reported to exhibit properties such as superhydrophobicity[4] and an extremely low optical reflectivity.[5] Moreover, VA-CNTs have been used as precursors of assemblies with different morphologies, including CNT yarns[6,7] and shape-controlled CNT agglomerates.[8,9]

Functionalization of the CNT sidewalls (including functionalization by chemical groups, deposition of nanoparticles, and heteroatom doping) can impart VA-CNTs with additional properties for various applications. Deposition of catalyst nanoparticles would enable VA-CNTs to be used as catalyst supports for fuel cells with improved mass transport paths and higher relative surface areas than conventional catalyst supports composed of carbon black.[3] Nitrogen doping of VA-CNTs has been reported to impart catalytic properties[10,11] and to alter the electronic states,[12] which opens up the possibility of controlling the electrical conductivity.

Functionalization of CNTs often accompanies solution-immersion processes, such as conventional impregnation-reduction process for catalyst deposition[3] and nitric acid pretreatment to produce oxidized CNTs (OCNTs) that are reactive with other chemical molecules.[13] However, agglomeration of CNTs, which is undesirable when the aligned morphology is to be advantageously utilized, has been observed during soaking of solution and solvent evaporation of these processes.

In the present paper, we review two methods that we previously developed for functionalizing the sidewalls of VA-CNTs, which have the ability to retain aligned morphology by preventing agglomeration. The first method involves deposition of Pt nanoparticles on VA-CNTs by utilizing antisolvent precipitation of

fine naphthalene particles, which may inhibit access of adjacent CNTs through surface tension.[14] The advantage of this method is demonstrated by comparing it with the conventional solution-immersion process, which caused severe agglomeration of VA-CNTs. The second method involves nitrogenation by applying pretreatment of ultraviolet light (UV) irradiation and subsequently reacting with ammonia gas; these vapor-phase processes did not cause agglomeration of VA-CNTs.[15] The chemical bonding states in nitrogenated VA-CNTs (VA-NCNTs) were investigated by spectroscopic analysis.

2. Experimental

2. 1 Preparation of VA-CNTs

VA-CNTs were synthesized by thermal chemical vapor deposition (CVD) according to the procedure described in our previous report.[16] 1 cm × 1 cm silicon substrates on which Fe–Ti–O catalyst nanoparticles had been dispersed were placed in the CVD chamber. VA-CNTs were grown on these substrates by heating them to 700°C and introducing a 10 sccm C_2H_2 and 20 sccm H_2 gas mixture to the CVD chamber. The outer diameters of individual CNTs were in the range 5–10 nm and heights of VA-CNTs were 80–300 μm.

2. 2 Development of Anti-agglomerating Method and its Application to Pt Deposition[14]

The VA-CNTs were subjected to processes I–III illustrated in **Scheme 1**. The developed anti-agglomerating method is referred to as process I. In process I, a 30-μL naphthalene (Nap)/ethanol (EtOH) solution (60 g L^{-1} Nap) was soaked into the VA-CNTs. A 40–60-μL water, an antisolvent of Nap, was then added to the soaked Nap/EtOH solution to precipitate Nap crystals. Then the EtOH and water were evaporated and the Nap crystals were sublimed by evacuation (<10 kPa). For comparison, we also employed process II, which induced capillary-driven agglomeration that gave a similar morphology to previously reported morphologies,[9] and process III, which had attempted to inhibit agglomeration by filling the intertube space with Nap crystals but caused agglomeration with a different morphology. In process II, a 30-μL EtOH was soaked into the VA-CNTs and then naturally evaporated. In process III, a 30-μL Nap/EtOH solution was soaked into the VA-CNTs, and the EtOH was then naturally evaporated to precipitate Nap crystals, which were subsequently sublimed by evacuation.

Utilizing process I, which exhibited the lowest degree of agglomeration of the above three processes, we deposited Pt nanoparticles on the sidewalls of VA-CNTs. A 30-μL $Pt[(NO_2)_2(NH_3)_2]HNO_3$/Nap/EtOH solution (0.989 g L^{-1} Pt, 60 g L^{-1} Nap) was soaked into VA-CNTs, water was added, EtOH and water were evaporated, and Nap crystals were sublimed. The sample was then annealed in an Ar–4%H_2 atmosphere at 200 °C for 120 min to reduce Pt(II) to Pt.

2. 3 Nitrogenation of VA-CNTs[15]

The VA-CNTs were first pretreated by UV irradiation to produce VA-OCNTs. UV light with wavelengths of 184.9 and 253.7 nm generated by a low-pressure mercury lamp was irradiated on the VA-CNTs in air for 30 min. UV irradiation in air has been considered to generate O_3 and atomic oxygen, which would oxidize the present VA-CNTs. VA-NCNTs were produced by reacting the VA-OCNTs with NH_3 by annealing VA-OCNTs in a 0.4 L min^{-1} NH_3 and 0.2 L min^{-1} Ar gas mixture at 600 °C for 1 h. During natural cooling from the annealing temperature to room temperature, the gas flow was changed from the NH_3–Ar mixture to 0.5 L min^{-1} Ar at 300 °C to

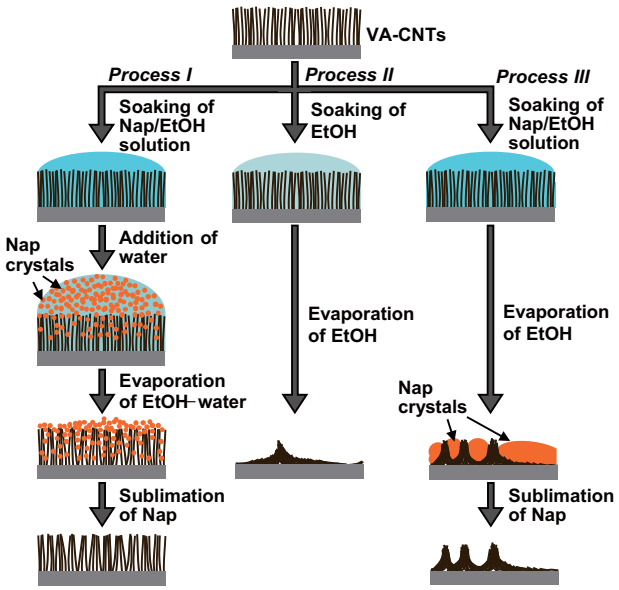

Scheme 1 Wetting/drying processes conducted on VA-CNTs.

desorb unreacted NH_3 molecules. For comparison, we also nitrogenated pristine VA-CNTs that had not been subjected to the UV pretreatment.

2. 4 Characterization of Pristine and Functionalized VA-CNTs

Secondary electron (SE) and backscattered electron (BE) images were acquired by field-emission scanning electron microscopy (FE-SEM). Optical micrographs were obtained using a stereoscopic microscope coupled with a halogen lamp. In transmission electron microscopy (TEM) observations, CNTs dispersed in EtOH by ultrasonication were dropped onto the TEM grid and the EtOH was then evaporated. X-ray photoelectron spectroscopy (XPS) was performed using a Mg Kα X-ray source. All binding energies were referenced to C 1s peak of graphite at 284.5 eV. Fourier-transform infrared spectroscopy (FT-IR) was performed by the attenuated total reflection method. Auger electron spectroscopy (AES) was used for elemental analysis of the surface and cross section of VA-NCNTs. Raman spectroscopy was performed by using the second harmonic of a Nd:YAG laser ($\lambda = 532$ nm) as the excitation light.

3. Results and Discussion

3. 1 Anti-agglomerating Deposition of Pt Nanoparticles on VA-CNTs[14]

Figures 1a–h show FE-SEM SE images of pristine VA-CNTs and VA-CNTs subjected to processes I–III. The pristine VA-CNTs consisted of a mixture of straight and wavy CNTs in which adjacent CNTs were partially contacted and the intertube spacing ranged up to several hundred nanometers (Fig. 1b).The vertical alignment was retained after process I (Fig. 1c) and only bundles were formed consisting of several CNTs (Fig. 1d). In contrast, the vertical alignment was severely disrupted after processes II and III. Process II caused the VA-CNTs to agglomerate into a reticular morphology that consisted of walls of vertically stood CNTs and interior areas of horizontally laid CNTs on the surface of substrate (Fig. 1e). Process III caused agglomeration with a different morphology that had porous areas with various sizes of pores and flat areas of horizontally laid CNTs (Fig. 1g). CNTs were densely packed after processes II (Fig. 1f) and III (Fig. 1h).

We also found that the anti-agglomerating effect of process I could be easily confirmed by optical micrographs, as shown in **Figs. 2**a–d. The pristine VA-CNTs appeared very dark (Fig. 2a) due to their low optical reflectance.[5] Most of the surface appeared dark after process I, indicating that the vertical alignment was extensively retained (Fig. 2b). In contrast, optical micrographs of the VA-CNTs subjected to processes II (Fig. 2c) and III (Fig. 2d) exhibit dark and light contrast patterns caused by agglomeration; the light regions in these patterns would correspond to areas of horizontally laid CNTs in FE-SEM images.

We consider that the antisolvent Nap precipitation step in process I is crucial for preventing

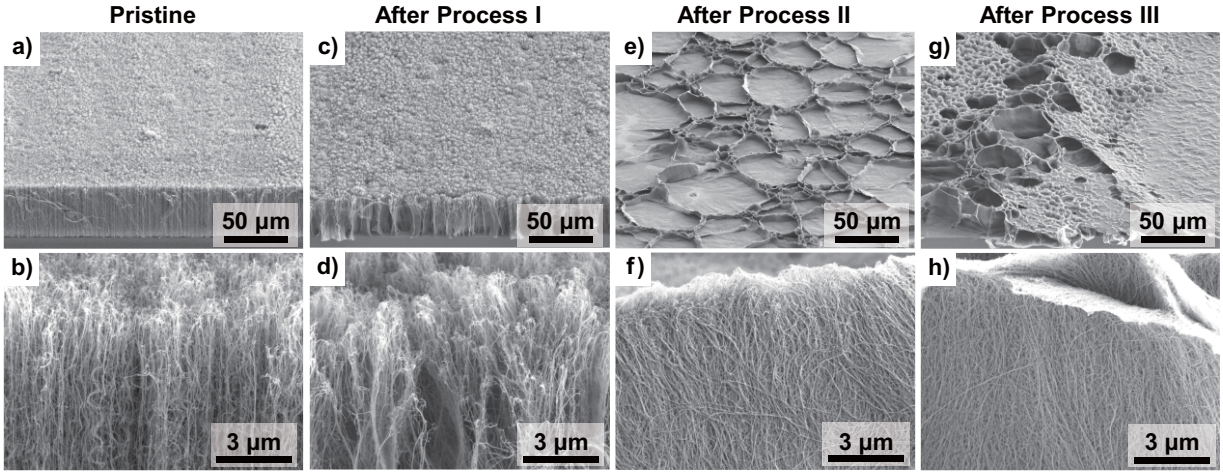

Fig. 1 FE-SEM SE images of VA-CNTs: (a, b) pristine VA-CNTs, VA-CNTs subjected to processes (c, d) I, (e, f) II, and (g, h) III. Top and bottom rows show low and high magnification images, respectively.

agglomeration. In process I, Nap crystals would precipitate as fine particles on water addition, since adding an antisolvent has been reported to result in rapid supersaturation of solutes and to precipitate solutes as fine particles.[17] These fine Nap particles were assumed to be incorporated in the intertube spaces to inhibit capillary-driven access of adjacent CNTs during EtOH evaporation. In process II in which Nap crystals were precipitated by EtOH evaporation, precipitation was initiated from a few nucleation points and thus Nap crystals grew significantly larger than the intertube spacing, disrupting the alignment of the CNTs.

While process I produced a lower degree of agglomeration than processes II and III, bundles of several CNTs were still observed. These bundles may form during EtOH–water evaporation because the Nap particles may be slightly larger than the intertube spacing or they may form during other steps, such as during the introduction of EtOH, which can also generate a capillary force, and during submersion in EtOH–water where intertube forces might act between adjacent CNTs. The degree of agglomeration during these steps may be influenced by the diameter and the height of VA-CNTs or the strength of adhesion to the substrate, which would affect the susceptibility of VA-CNTs to capillary and intertube forces. For example, liquid introduction has been reported to reduce the lateral dimension of vertically aligned single-walled CNTs by ~20%.[8] Therefore, the present anti-agglomerating method, which can inhibit agglomeration only during the solvent evaporation step, may not be applicable to all types of VA-CNTs.

Figures 3a–c show FE-SEM SE and BE images of VA-CNTs that had been deposited with Pt nanoparticles by applying the anti-agglomerating method. The SE images indicate that the vertical alignment was retained (Fig. 3a) and that agglomeration of CNTs was significantly inhibited (Fig. 3b). The BE image (Fig. 3c) reveals deposition of nanoparticles with diameters less than 5 nm, which were composed of elements heavier than carbon. **Figure 4** shows typical TEM images of CNTs after Pt deposition. The lattice fringe of the nanoparticles had a periodicity of 0.23 nm, which

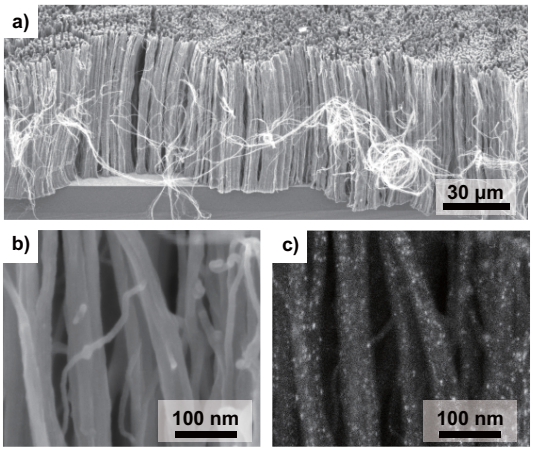

Fig. 3 FE-SEM images of VA-CNTs deposited with Pt nanoparticles: (a) low- and (b) high-magnification SE images; (c) BE image corresponding to high-magnification SE image in (b).

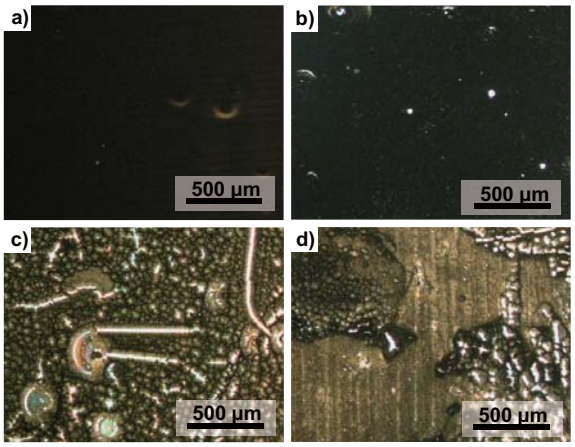

Fig. 2 Optical micrographs of VA-CNTs: (a) pristine VA-CNTs, VA-CNTs subjected to processes (b) I, (c) II, and (d) III.

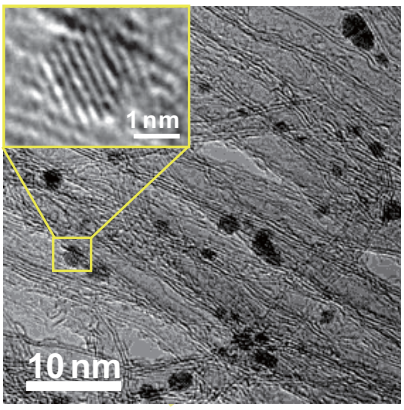

Fig. 4 Typical TEM images of CNTs deposited with Pt nanoparticles. Inset: high-resolution TEM image of a Pt nanoparticle in which lattice fringes are visible.

corresponds to the lattice spacing of the Pt(111) plane, implying that the nanoparticles in the BE image would consist of Pt. The CNTs with Pt nanoparticles in the TEM images are densely packed due to agglomeration during the EtOH evaporation step when loading them onto the TEM grid.

3. 2 Nitrogenation of VA-CNTs[15]

Figure 5a presents a flow diagram of the experiments and the compositions obtained by XPS. Considerably more nitrogen atoms were incorporated in VA-NCNTs than in the sample nitrogenated without UV pretreatment. Figures 5b and c respectively show O 1s and N 1s XPS spectra of obtained samples. The O 1s spectrum of VA-OCNTs contained two peaks at around (O-1) 532.0 and (O-2) 533.5 eV. These peaks have been respectively assigned to (O-1) C=O[18] and (O-2) C−O.[18] The intensities of these peaks in the O 1s spectrum of VA-NCNTs were lower than those in the O 1s spectrum of VA-OCNTs, implying that chemical groups containing C=O and C−O bonds decreased by reacting with NH_3. The N 1s spectrum of VA-NCNTs contained four peaks at around (N-1) 398.3, (N-2) 399.7, (N-3) 401.0, and (N-4) 403.9 eV. The first three peaks have been respectively assigned to (N-1) pyridinic sites,[19,20] (N-2) pyrrolic sites,[19] and (N-3) quaternary sites.[19,20] Peaks (N-1) and (N-2) had higher intensities than peak (N-3), indicating that there were more nitrogen atoms at pyridinic and pyrrolic sites than at quaternary sites. The last peak would be assigned to (N-4) oxides or shake-up satellites originating from π bonds in the heteroaromatic rings.

Figure 6 shows IR difference spectra of OCNTs and NCNTs obtained by subtracting the IR spectrum of pristine CNTs. Bands at around (i) 1000–1200, (ii) 1500–1600, (iii) 1600–1700, and (iv) 3000–3500 cm^{-1} appeared in the IR difference spectrum of OCNTs. These bands have been respectively assigned to (i) υC−O−C, (ii) IR-activated υC=C, (iii) υC=O, and (iv) υO−H.[21] In the IR difference spectrum of NCNTs, bands (iii) and (iv) did not appear and the intensity of band (ii) shoulder at around 1500–1580 cm^{-1} was greater than that in the spectrum of OCNTs. Band (ii) shoulder was located close to a previously reported band that has been assigned to the heteroaromatic ring of graphitic carbon nitride.[22] Therefore, the C=O and C−OH groups in OCNTs were assumed to react with NH_3, introducing nitrogen covalently as heteroatoms in the aromatic rings composing the tube framework. The intensity of band (i) in the spectrum of NCNTs was similar to that in the spectrum of OCNTs, implying that the C=O and C−OH groups may be more reactive to NH_3 than the C−O−C groups.

Figures 7a and b show Raman spectra of pristine CNTs and NCNTs, respectively. The D and G bands in

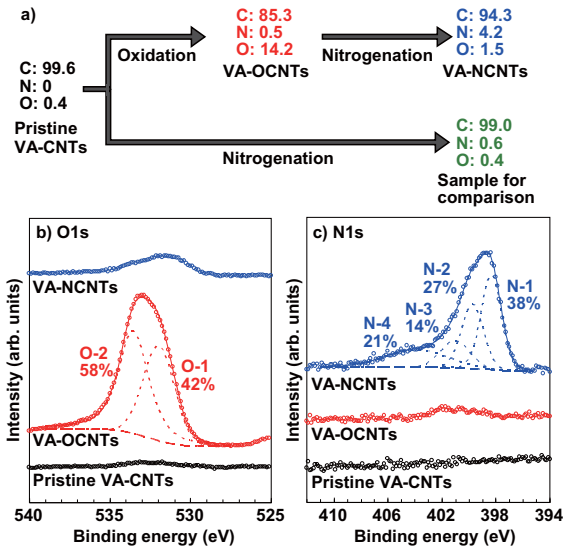

Fig. 5 (a) Flow diagram of experiments. XPS atomic ratios C/N/O. (b) O 1s and (c) N 1s XPS spectra of obtained samples. Ratios of peak areas are also shown.

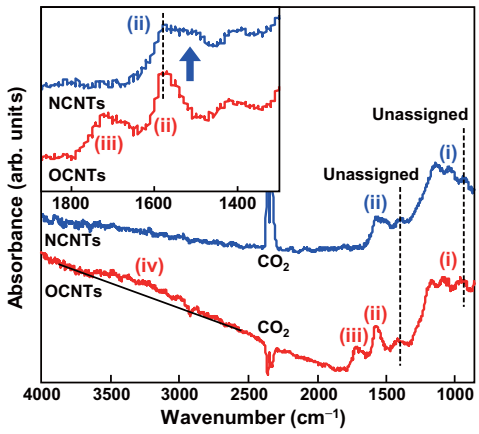

Fig. 6 IR difference spectra of OCNTs and NCNTs obtained by subtracting IR spectrum of pristine CNTs. Inset shows same spectra in which the wavenumber region near bands (ii) and (iii) is enlarged to clearly show the reduction in band (iii) and the increase in band (ii) shoulder (indicated by blue arrow).

the Raman spectra of pristine CNTs and NCNTs had intensity ratios (I_D/I_G) of 1.0 and 1.4, respectively. The increase in I_D/I_G on nitrogenation would indicate that disorder in the tube structure was promoted, and may be related to the reduction of the size of the ordered sp^2 domains in CNTs, since I_D/I_G has been reported to be inversely proportional to the in-plane crystallite size in nanographite[23] and in CNTs.[24] Despite promoting disorder in the tube structure, the cylindrical structure was preserved even after nitrogenation, as observed by TEM (**Fig. 8**), which is significant because it has been difficult to synthesize NCNTs with cylindrical structures directly from precursors containing nitrogen and carbon.

Figures 9a–d show typical AES derivative spectra collected from upper, middle, and lower regions of the cross section and the surface of VA-NCNTs, respectively. The presence of a peak assigned to nitrogen in all four spectra reveals that nitrogen atoms were incorporated throughout the entire sidewalls and tube-ends of the VA-NCNTs. The higher concentration of nitrogen atoms near the surface than those of the other regions may be attributed to one of the following reasons: (1) high reactivity of the tube-ends to oxidizing species generated during UV irradiation or to NH_3 molecules, (2) high UV absorption at the near-surface region of VA-CNTs, or (3) a concentration gradient of oxidizing species or NH_3 molecules.

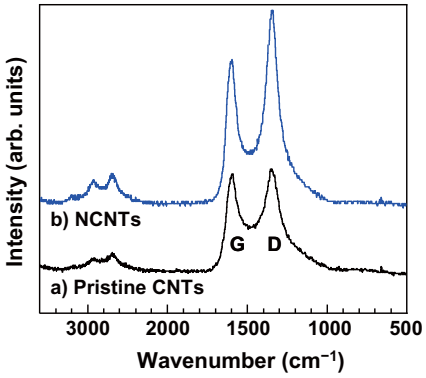

Fig. 7 Raman spectra of (a) pristine CNTs and (b) NCNTs.

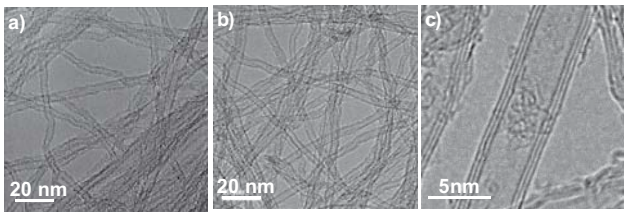

Fig. 8 Typical TEM images of (a) pristine CNTs and (b) NCNTs and (c) high-magnification TEM image of NCNTs.

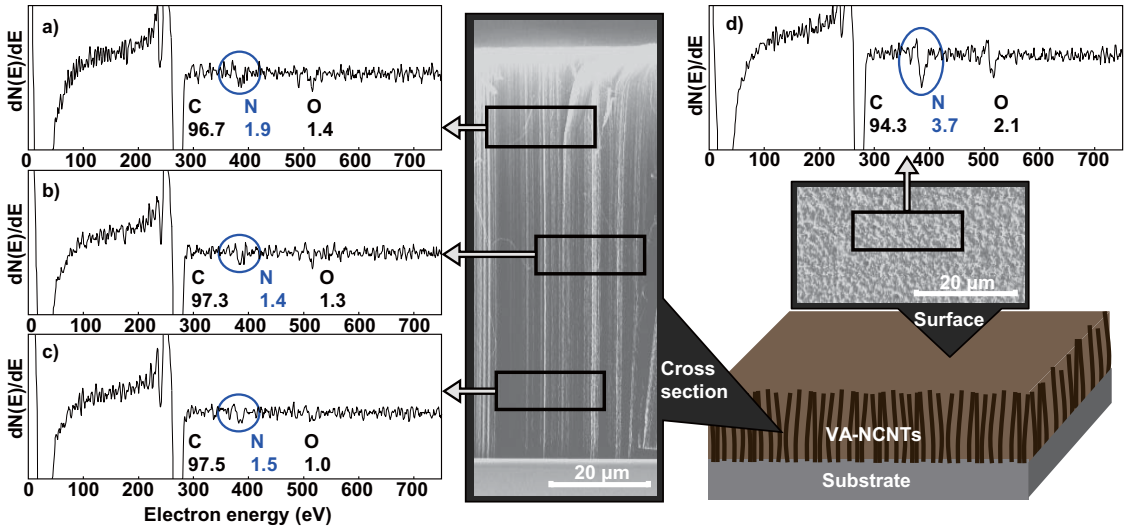

Fig. 9 FE-SEM SE images of (left) cross section obtained by cleaving and (right) surface of VA-NCNTs. Typical AES derivative spectra collected from square areas on (a) upper, (b) middle, and (c) lower regions of cross section and (d) surface region. AES atomic ratios C/N/O are given. Blue circles indicate nitrogen peaks.

We also confirmed that NCNT yarns can be prepared by this nitrogenation process, either by dry-spinning VA-NCNTs or by nitrogenating already-spun CNT yarns. We discussed the correlation between the chemical bonding states and the electrical conductivity of NCNT yarns in our previous study.[15]

4. Conclusions

We have developed two new methods for functionalizing the sidewalls of VA-CNTs, which were capable of avoiding disruption of the aligned morphology. The first method utilized dissolution and antisolvent precipitation of Nap to preserve the vertical alignment of CNTs during desiccation of wet VA-CNTs. We applied this inexpensive and straightforward method to deposit Pt nanoparticles on the sidewalls of VA-CNTs. The second method produced VA-NCNTs without destroying the alignment by all-vapor-phase nitrogenation utilizing UV pretreatment. Spectroscopic analysis revealed that this process incorporated nitrogen atoms at mainly pyridinic and pyrrolic sites. We anticipate that VA-NCNTs will be used in applications such as highly reactive catalysts by exploiting the catalytic activities of pyridinic sites.[11]

Acknowledgements

The authors thank Dr. Siry, M. at DENSO CORPORATION for helpful discussions. The functionalized VA-CNTs were characterized with assistance from our collaborators at TCRDL, namely Mr. Seki, J. (FE-SEM), Mr. Suzuki, N. (TEM), Mr. Sudo, E. (Raman spectroscopy), Ms. Takahashi, N. (XPS), and Mr. Kimoto, Y. (AES).

We are also grateful to the publisher for giving us permission to adapt the following figures:

Scheme 1 and Figures 1-4: Adapted from Ohta, R., et al., Chem. Commun., Vol. 46 (2010), pp. 5259-5261, by permission of The Royal Society of Chemistry.

Figures 5-9: Adapted from Ohta, R., et al., Chem. Commun., Vol. 47, No. 13 (2011), pp. 3873-3875, by permission of The Royal Society of Chemistry.

References

(1) (a) Thostensona, E. T., et al., "Advances in the Science and Technology of Carbon Nanotubes and their Composites: a Review", *Comp. Sci. Technol*., Vol. 61, No. 6348 (1991), pp. 56-58;
(b) Saito, R., et al., *Physical Properties of Carbon Nanotubes* (1998), Imperial College Press.

(2) (a) Choi, W. B., et al., "Fully Sealed, High-brightness Carbon-nanotube Field-emission Display", *Appl. Phys. Lett*., Vol. 75, No. 20 (1999), pp. 3129-3131;
(b) Fan, S., et al., "Self-Oriented Regular Arrays of Carbon Nanotubes and Their Field Emission Properties", *Science*, Vol. 283, No. 5401 (1999), pp. 512-514.

(3) Hatanaka, T., et al., "PEFC Electrodes Based on Vertically Oriented Carbon Nanotubes", *ECS Transactions*, Vol. 3, No. 1 (2006), pp. 277-284.

(4) Lau, K. K. S., et al., "Superhydrophobic Carbon Nanotube Forests", *Nano Lett*., Vol. 3, No. 12 (2003), pp. 1701-1705.

(5) Yang, Z. -P., et al., "Experimental Observation of an Extremely Dark Material Made by a Low-density Nanotube Array", *Nano Lett*., Vol. 8, No. 2 (2008), pp. 446-451.

(6) Zhang, M., et al., "Multifunctional Carbon Nanotube Yarns by Downsizing an Ancient Technology", *Science*, Vol. 306, No. 5700 (2004), pp. 1358-1361.

(7) Oshima, H., et al., "Reduction of the Electrical Resistance of Carbon Nanotube Yarns by Chemical Treatments", *Abstracts of the 39th Fullerenes-nanotubes General Symposium*, (2010), p. 70.

(8) Futaba, D. N., et al., "Shape-engineerable and Highly Densely Packed Single-walled Carbon Nanotubes and their Application as Super-capacitor Electrodes", *Nature Mater*., Vol. 5 (2006), pp. 987-994.

(9) Liu, H., et al., "Self-assembly of Large-scale Micropatterns on Aligned Carbon Nanotube Films", *Angew. Chem. Int. Ed*.,Vol. 43, No. 9 (2004), pp. 1146-1149.

(10) Gong, K., et al., "Nitrogen-doped Carbon Nanotube Arrays with High Electrocatalytic Activity for Oxygen Reduction", *Science*, Vol. 323, No. 5915 (2009), pp. 760-764.

(11) (a) Rao, C. V., et al., "In Search of the Active Site in Nitrogen-doped Carbon Nanotube Electrodes for the Oxygen Reduction Reaction", *J. Phys. Chem. Lett*., Vol. 1, No. 18 (2010), pp. 2622-2627;
(b) van Dommele, S., et al., "Nitrogen-containing Carbon Nanotubes as Solid Base Catalysts" *Chem. Commun*., No. 46 (2006), pp. 4859-4861.

(12) (a) Kaun, C. C., et al., "Current-voltage Characteristics of Carbon Nanotubes with Substitutional Nitrogen", *Phys. Rev. B*, Vol. 65, No. 20 (2002), 205416;
(b) Czerw, R., et al., "Identification of Electron Donor States in N-doped Carbon Nanotubes", *Nano Lett*., Vol. 1, No. 9 (2001), pp. 457-460.

(13) Worsley, K. A., et al., "Functionalization and Dissolution of Nitric Acid Treated Single-walled Carbon Nanotubes", *J. Am. Chem. Soc*., Vol. 131, No. 50 (2009), pp. 18153-18158.

(14) Ohta, R., et al., "Anti-agglomerating Effect in

Vertically Aligned Carbon Nanotubes derived by Antisolvent Precipitation of Naphthalene", *Chem. Commun*., Vol. 46, No. 29 (2010), pp. 5259-5261.
(15) Ohta, R., et al., "Alignment-retainable Nitrogenation of Cylindrical Carbon Nanotubes by Thermal Reaction with Ammonia Following UV Oxidation: Chemical Alteration Effects on Electrical Conductivity", *Chem. Commun*., Vol. 47, No. 13 (2011), pp. 3873-3875.
(16) Gunjishima, I., et al., "Growth of Vertically Aligned Carbon Nanotubes from Highly Active Fe–Ti–O Nanoparticles Prepared by Liquid-phase Synthesis", *Jpn. J. Appl. Phys*., Vol. 46, No. 6A (2007), pp. 3700-3703.
(17) (a) Kasai, K., et al., "A Novel Preparation Method of Organic Microcrystals", *Jpn. J. Appl. Phys*., Vol. 31, No. 8A (1992), pp. L1132-L1134;
(b) van Keuren, E., et al., "Kinetics of the Formation of Organic Molecular Nanocrystals", *Nano Lett*., Vol. 1, No. 3 (2001), pp. 141-144.
(18) Okpalugo, T. I. T., et al., "High Resolution XPS Characterization of Chemical Functionalised MWCNTs and SWCNTs", *Carbon*, Vol. 43, No. 1 (2005), pp. 153-161.
(19) Ripalda, J. M., et al., "Correlation of X-ray Absorption and X-ray Photoemission Spectroscopies in Amorphous Carbon Nitride", *Phys. Rev. B*, Vol. 60, No. 6 (1999), pp. R3705-R3708.
(20) Casanovas, J., et al., "Origin of the Large N 1s Binding Energy in X-ray Photoelectron Spectra of Calcined Carbonaceous Materials", *J. Am. Chem. Soc*., Vol. 118, No. 34 (1996), pp. 8071-8076.
(21) Mawhinney, D. B., et al., "Infrared Spectral Evidence for the Etching of Carbon Nanotubes: Ozone Oxidation at 298 K", *J. Am. Chem. Soc*., Vol. 122, No. 10 (2000), pp. 2383-2384.
(22) (a) Guo, Q., et al., "Synthesis of Carbon Nitride Nanotubes with the C_3N_4 Stoichiometry via a Benzene-thermal Process at Low Temperatures", *Chem. Commun*., No. 1 (2004), pp. 26-27;
(b) Khabashesku, V. N., et al., "Powder Synthesis and Characterization of Amorphous Carbon Nitride", *Chem. Mater*., Vol. 12, No. 11 (2000), pp. 3264-3270.
(23) (a) Matthews, M. J., et al., "Origin of Dispersive Effect of the Raman D Band in Carbon Materials", *Phys. Rev. B*, Vol. 59, No. 10 (1999), pp. R6585-R6588;
(b) Cançado, L. G., et al., "General Equation for the Determination of the Crystallite Size La of Nanographite by Raman Spectroscopy", *Appl. Phys. Lett*., Vol. 88, No. 16 (2006), 163106.
(24) Soin, N., et al., "Excitation Energy Dependence of Raman Bands in Multiwalled Carbon Nanotubes", *J. Raman Spectrosc*., Vol. 41, No. 10 (2010), pp. 1227-1233.

Riichiro Ohta
Research Fields:
- Surface Finishing
- Synthesis and Characterization of Carbon-based Materials

Academic Degree: Dr.Eng.
Academic Societies:
- The Japan Society of Applied Physics
- The Electrochemical Society of Japan

Award:
- ECS-sponsored Young Researcher Award, Tokai Branch of the Electrochemical Society of Japan, 2011

Itaru Gunjishima
Research Fields:
- Silicon Carbide
- Carbon Nanotube
- Nanoparticle

Academic Degree: Dr.Eng.
Academic Society:
- The Japan Society of Applied Physics

Tomohiro Shimazu*
Research Field:
- Heat Exchanger

Hisayoshi Oshima*
Research Field:
- Nano-carbon Materials

Academic Degree: Dr.Eng.
Academic Societies:
- The Japan Society of Applied Physics
- The Surface Science Society of Japan
- The Carbon Society of Japan

Kazuma Shinozaki
Research Field:
- Polymer Electrolyte Fuel Cells

Academic Society:
- The Electrochemical Society of Japan

Koichi Nishikawa
Research Fields:
- Semiconductor Power Device
- Power Electronics

Academic Degree: Dr.Eng.
Academic Societies:
- The Japan Society of Applied Physics
- The Japanese Association for Crystal Growth

*DENSO CORPORATION

Hatanaka Tatsuya

Research Fields:
- Electrochemical Materials
- Solid State Physics

Academic Societies:
- The Electrochemical Society
- The Electrochemical Society of Japan
- Catalysis Society of Japan

Atsuto Okamoto

Research Fields:
- Surface and Coatings Technology
- Synthesis and Characterization of Nanocarbons

Academic Societies:
- The Japan Society of Applied Physics
- The Japanese Association for Crystal Growth
- The Carbon Society of Japan

Award:
- The 32nd National Conference on Crystal Growth Incentive Award, the Japanese Association for Crystal Growth, Japan, 2002

